Satellight
Commission of the European Communities

DNMI

Fifth SATELLIGHT meeting, Sophia Antipolis November 27-28 1997

SATELLITE DERIVED AND GROUND TRUTH HORIZONTAL AND VERTICAL ILLUMINANCE/IRRADIANCE FROM THE IDMP STATIONS AT GENEVA AND GÄVLE

by

Arvid Skartveit and Jan Asle Olseth

SATELLIGHT Programme JOR3-CT950041
First draft, November 1997

1. INTRODUCTION

Most radiation-driven processes are spectrally selective, like the photosynthesis or the erythemal response of human skin to ultraviolet radiation. Equally well-known is the concept of daylight, i.e. solar radiation evaluated in proportion to its capability of stimulating the human eye. Even though daylight data are in great demand, they frequently have to be estimated from prescribed luminous efficacies and observed or estimated beam and diffuse irradiance.

In previous notes (Skartveit & Olseth, 1996a, b, Skartveit & Olseth, 1997, Olseth & Skartveit, 1997b) it has been shown that both horizontal and vertical illuminances can be estimated with high precision from surface based horizontal irradiance. This has been done both for the two International Daylight Measuring Programme (IDMP) stations involved in the present note (Geneva and Gävle) and for the IDMP stations at Lisbon and Lyon.

The present note first demonstrates how well horizontal irradiances are estimated from Meteosat data using Heliosat Versions 7, 8, and 9, and then it deals with how well horizontal and vertical illuminances can be estimated from these Meteosat horizontal irradiances by a luminous efficacy algorithm and a slope algorithm.

2. DATA

2.1 Meteosat / Heliosat irradiation data

The Heliosat procedure is described by Beyer et al. (1996). A measure of cloud cover is inferred from pixel counts in the VIS-channel (0.5 - 0.9 μm), and this measure is subsequently used to estimate surface global irradiance as a fraction of the irradiance under clear sky conditions. This procedure is carried out with one clear sky model, viz. the Kasten/Dumortier model with Linke turbidity coefficient 3.0. As shown in Olseth & Skartveit (1997a) the Kasten/Dumortier clear sky model and the McMaster model (Davies & McKay, 1989) with estimated climatological water vapour and turbidity as input, yield nearly identical cloud free global irradiances. These modelled values also agree nicely with observed cloud free irradiances at Bergen.

For Geneva and Gävle, global radiation data for 3 X 5 pixels centred around the ground pixel of the station, were estimated by the Heliosat procedure (Versions 7, 8, and 9) from Meteosat image acquisition each half hour (Hammer 1997). Based on these global radiation data, horizontal diffuse radiation is estimated by the Skartveit & Olseth diffuse fraction model (1987). By using a recent modification of this diffuse fraction model (Skartveit et al., 1997) only moderate changes in the satellite derived slope illuminances were obtained.

2.2 Ground truth irradiation and illumination data

Surface data from the Swiss Research class IDMP station at Geneva (46°12'N, 6°06'E, 425 m above m.s.l.; April 1994 - March 1995) were gratefully received from Pierre Ineichen at GAP-Energie, Universite de Geneve, while data from the Swedish General class station at Gävle (60°40'N, 17°10'E, 16 m above m.s.l.; April-December 1995) were gratefully received from H. A. Löfberg at the Royal Institute of Technology, Department of Built Environment.

At Geneva, global and diffuse horizontal irradiances are measured by Kipp&Zonen CM11 pyranometers, while normal beam irradiance is measured by a Eppley NIP. Global and vertical illuminances (towards North, East, South, and West) are measured by PRC910GV, diffuse horizontal illuminance by a LiCor instrument, and normal beam illuminance is measured by a LiCor instrument

with tube. The sensors for diffuse irradiance/illuminance are shaded with shadow rings (8 cm width, 40 cm radius. The data used in this paper are ten minute averages (± 5 min around the hours of Meteosat data).

At Gävle, global and diffuse horizontal irradiances are measured by Kipp&Zonen CM11 pyranometers, while horizontal and vertical illuminances are measured by Licor LI-210 SZ sensors. The sensor for diffuse irradiance/illuminance are shaded by a sun tracking shading disk (7 cm radius, 70 cm distance). The data used in this paper are hourly averages.

For both stations, ground reflected radiation is screened off from the vertical sensors by a black screen (honeycomb) which apparently provides a foreground albedo ≈ 0.1 (see Chapter 3.2).

2.3 Comparison between Meteosat / Heliosat and ground truth irradiation data

We express the global irradiance in terms of clear sky index k_g , which is the ratio between actual global irradiance (observed or satellite derived) and cloudless global irradiance, estimated by the Kasten/Dumortier model with Linke turbidity coefficient 3.0.

Frequency distributions (Fig. 1a) of half-hourly global clear sky indices (surface observed and Heliosat Versions 7, 8, and 9) at Geneva reveal that in the summer months the high clear sky index mode of these Heliosat Versions is more significantly shifted towards higher values relative to the surface observed counterpart than what is the case at Gävle and 8 other high latitude stations (Olseth & Skartveit, 1997c).

"Percentile match curves", which relate clear sky indices k_g and cloud indices n are plotted as follows: the lowest k_g against the highest n, the second lowest k_g against the second highest n, ... the highest k_g against the lowest n. Such ground truth curves, plotted for the central 95% of the distributions, deviate from the straight line $\mathbf{k_g = 1 - n}$, applied in the Heliosat Versions, both for the summer and the winter period at Geneva (Figs. 2a and b). For snow-free periods at Gävle (Fig. 2c), as for the other 8 high latitude stations in Olseth & Skartveit (1997c), the ground truth percentile match curves are, however, close to this straight line, at least for Versions 7 and 8. For Geneva the solar elevation dependency of the observations vs. Heliosat conformity is small for all Versions, at least for solar elevations > 20^o (Figs. 2a and b). For Gävle, as for the 8 other high latitude stations (Olseth & Skartveit, 1997c), this solar elevation conformity is least for Version 8 (Fig. 2c), in which case it is close to negligible for solar elevations > 20^o.

It is noteworthy, however, that the ground truth vs. Heliosat conformity at Geneva is significantly improved if the Heliosat cloud indices n are kept unchanged while cloudless global irradiation is calculated from climatological monthly Linke turbidities from Geneva, rather than from a fixed Linke turbidity = 3.0. This improvement is shown for Version 8 (V8*) as an example in Figs. 1b, 2a-b). Moreover, this improvement is particulary pronounced in summer, when actual turbidities exceed 3.0 most significantly.

3. MODELS

3.1 The luminous efficacy model

The luminous efficacy model (Olseth & Skartveit, 1989) is based on the CIE curve for photopic vision and spectral irradiances obtained by an interpolation between transmittance models for, respectively, cloudless sky (Bird & Riordan, 1986) and unbroken cloud cover (Stephens et al, 1984). This interpolation decomposes the diffuse irradiance into "blue sky", "dark cloud", and "bright cloud"

irradiance. For partly cloudy cases, the model was slightly tuned to hourly global illuminance and irradiance from Bergen. The parameterized version of the model requires solar elevation, day of year, and diffuse and beam clearness indices as input. In the case of beam irradiation, the model is slightly modified here to explicitly account for variation in column amount of water vapour, under the assumption that water vapour extinction takes place solely at non-visible wavelengths. Moreover, in the case of diffuse irradiation the model is tuned to data from Albany, NY (gratefully received from R. Perez) by multiplying the difference between "dark cloud" efficacy and extraterrestrial efficacy by a factor 0.7. For Geneva the luminous efficacy model is run with the climatological average monthly water vapour amounts (WMO, 1982). Since Gävle and Bergen are at the same latitude, the model is run with the same monthly water vapour amounts as those estimated for Bergen (0.8-1.9 cm).

3.2 The slope algorithm

Given horizontal beam irradiance/illuminance, the beam irradiance/illuminance on a given slope is readily computed. To calculate the diffuse slope irradiance/illuminance requires additional information about surface reflectance and the horizontal diffuse sky irradiance/illuminance and its angular distribution.

We apply our slope algorithm (Skartveit & Olseth, 1986) for diffuse irradiance even for diffuse illuminance. This algorithm assumes Lambertian ground reflectance and may account for local horizon effects. Sky radiance anisotropy for cloudless as well as overcast skies is parameterized as follows:

- One fraction, equal to the beam transmittance, of the horizontal diffuse irradiance is treated as circumsolar radiation (Hay, 1979).
- Another fraction, decreasing from 0.3 at overcast to zero at beam transmittance = 0.15, is treated as collimated radiation from the zenith.
- The remaining horizontal diffuse irradiance is treated as isotropic sky radiance.

In previous notes (Skartveit & Olseth, 1996 a, b, Skartveit & Olseth, 1997, Olseth & Skartveit, 1997b) it is strongly indicated that the horizontal foreground (honeycomb) of the vertical sensors is more close to having albedo A = 0.1 than to being completely black (A = 0.0). We therefore use foreground Lambertian albedo A = 0.1 for slope calculations in the following.

4. MODELLED VERSUS OBSERVED ILLUMINANCE.

"Modelled" horizontal diffuse/beam illuminance is obtained by transforming horizontal diffuse/beam irradiance into illuminance by the luminous efficacy model (Olseth & Skartveit, 1989). "Modelled" vertical illuminance is obtained by first transforming horizontal diffuse/beam irradiance into slope irradiance using the slope algorithm (Skartveit & Olseth, 1986). This slope irradiance is subsequently transformed into slope illuminance by the luminous efficacy model (Olseth & Skartveit, 1989) under the assumption that all components of the diffuse irradiance have the same luminous efficacy as the bulk horizontal diffuse sky irradiance.

With surface observed horizontal irradiances as model input there is a nice agreement between modelled and observed global illuminance, both for Geneva and Gävle (Figs. 3a and 4a). For Geneva we see a slight model surplus for horizontal beam and a similar model deficit for horizontal diffuse (Fig. 3a). For Gävle there is a model deficit for horizontal beam, while the model deficit for diffuse is only negligible (Fig. 4a). Both for horizontal and vertical surfaces, the scatter (model vs observed) increases substantially when the model input is changed from surface observed horizontal irradiances to Heliosat Version 8 global irradiances (Figs. 3 and 4).

Note, however, that these input dependent differences in model versus ground truth conformity (Figs. 3 and 4), are far less pronounced when corresponding percentile match curves are compared (Fig. 5). Figs. 3 - 5 thus imply the important fact that although the satellite derived illuminances do not match ground truth data perfectly on an hour by hour basis, their frequency distribution is close to the distribution of illuminances derived from ground truth horizontal irradiances and even to the distribution of ground truth illuminances.

It should also be noted that the non-linearity of the Geneva percentile match curves relating clear sky indices in Figs. 2a-b) is no longer seen in the corresponding curves relating illuminances in Figs. 5a-b). This removal of non-linearity is due to the fact that Fig. 2 and Fig. 5 account for solar elevation in different ways.

Averages of modelled (4 model input) and ground truth illuminance (global, diffuse, beam, $S90^o$, $W90^o$, $E90^o$, $N90^o$), and corresponding MBD (Mean Bias Deviation) and RMSD (Root Mean Squared Deviation) are listed in Tables 1 - 2. Some of these numbers are even plotted in Fig. 6. The MBD range at Gävle is some ± 5% of the global illuminance, fairly independent of the kind of input data used. A similar MBD range is even seen at Geneva for illuminances derived from ground truth irradiances, while a substantially wider MBD range is seen for Heliosat derived illuminances there. However, if climatological monthly Linke turbidities are used, instead of the fixed value 3.0, the MBD range for Version 8 is well within the ± 5% range even at Geneva, both is summer and in winter (Fig. 6b).

However, the south facing vertical in winter is an exception to this latter statement, reflecting the high sensitivity of south vertical illuminance to errors in the global irradiance estimate (Heliosat) at low solar elevation (Dec. - March) at Geneva (Fig. 6a-b, bottom left). As also seen in Figs. 3 and 4, note again the increase in RMSD when the input is changed from ground truth irradiances to Heliosat irradiances (Fig. 6a-b, right).

5. CONCLUDING REMARKS

During the summer months at Geneva, Heliosat Versions 7, 8, and 9 yield global irradiances under cloudless sky (or nearly so) which significantly exceed those observed, while the corresponding Heliosat versus ground truth controversy is only minor at Gävle. Moreover, this controversy is almost completely removed even at Geneva if cloudless global radiation is derived from climatological monthly Linke turbidities (instead of the fixed value 3.0 throughout the whole year) along with the Heliosat cloud indices.

For 4 model input and 7 illuminances, the MBD range at Gävle is some ± 5% of the global illuminance, fairly independent of the kind of input data used. A similar MBD range is even seen at Geneva for illuminances derived from ground truth irradiances, while a substantially wider MBD range is seen there for Heliosat derived illuminances. However, if climatological monthly Linke turbidities are used, the MBD range for even Version 8 is well within the ± 5% range at Geneva, both is summer and in winter.

RMSD increases significantly when the input to the luminous efficacy / slope model is changed from ground truth irradiances to Heliosat irradiances. Nevertheless, although satellite derived illuminances from Geneva and Gävle thus do not match ground truth data perfectly on an hour by hour basis, their frequency distribution is close to the distribution of illuminances derived from ground truth horizontal irradiances and even to the distribution of ground truth illuminances.

6. REFERENCES

H.G. Beyer, C. Costanzo and D. Heinemann (1996): Modifications of the Heliosat procedure for irradiance estimates from satellite images. Solar Energy **56**, 207 - 212.

R.E. Bird and C. Riordan (1986): Simple solar spectral model for direct and diffuse irradiance on horizontal and tilted planes at the earth's surface for cloudless atmospheres. J. Climate Appl. Meteor. 25, 87.

A. Hammer (1997): Satellite-derived global radiation data kindly submitted.

J.E. Hay (1979): Study of shortwave radiation on non-horizontal surfaces. Report No 79-12, Atmospheric Environment Service, Downsview, Ontario

J.A. Olseth and A. Skartveit (1989): Observed and modelled luminous efficacies under arbitrary cloudiness. Solar Energy 42, 221-233.

J.A. Olseth and A. Skartveit (1997a): High latitude global and diffuse radiation estimated from Heliosat. Report to Fourth SATELLIGHT meeting, Oldenburg June 5-6, 1997.

J.A. Olseth and A. Skartveit (1997b): Horizontal and vertical illuminance/irradiance from 4 IDMP stations. Report to Fourth SATELLIGHT meeting, Oldenburg June 5 - 6 1997.

J.A. Olseth and A. Skartveit (1997c): High latitude global and diffuse radiation estimated from Heliosat-Versions 7, 8, 9, and 10. Report to Fifth SATELLIGHT meeting, Sophia Antipolis November 27-28, 1997.

A. Skartveit and J.A. Olseth (1986): Modelling slope irradiance at high latitudes. Solar Energy 36, 333-344.

A. Skartveit and J.A. Olseth (1994): Luminous efficacy models and their application for calculation of photosynthetically active radiation. Solar Energy 52, 391-399.

A. Skartveit and J.A. Olseth (1996a): Illuminance/irradiance at a high latitude IDMP station. Report to Second SATELLIGHT meeting, Bergen June 24-25, 1996.

A. Skartveit and J.A. Olseth (1996b): Test of a luminous efficacy model on illuminance/irradiance data from 4 European IDMP stations. First draft (November 1966) prepared for the third SATELLIGHT meeting, Les Marecotte January 16-17, 1997.

A. Skartveit and J.A. Olseth (1997): Horizontal and vertical illuminance/irradiance from the IDMP station in Geneva. Report to Third SATELLIGHT meeting, Les Marecottes January 16/17 1997

A. Skartveit, J.A. Olseth and M.E. Tuft (1997): The potential for improvement of hourly diffuse fraction models. Submitted to Solar Energy, October 1997.

G.L. Stephens, S. Ackerman and E.A. Smith (1984): A short-wave parameterization revised to improve cloud absorption. J. Atmos. Sci. 41, 687.

World Meteorological Organization (1982): Climatological normals (CLINO) for climate and climate ship stations for the period 1931-1960. WMO/OMM-No.117.

GENEVA (MOD. = SURFACE)								
		N	OBS.	MOD.	MBD	RMSD	MBD	RMSD
			(klux)		(klux)		(%)	
YEAR	Global	4096	31.4	30.6	-0.8	1.7	-2.5	5.3
	Diffuse	4096	18.9	17.4	-1.5	3.1	-4.9	9.9
	Beam	4096	12.4	13.2	0.8	2.1	2.4	6.7
	S90	4096	20.3	19.7	-0.6	3.8	-2.0	12.2
	W90	4096	14.8	14.3	-0.5	3.0	-1.6	9.4
	E90	4096	13.6	12.8	-0.8	3.4	-2.5	10.8
	N90	4096	7.3	7.7	0.4	2.1	1.3	6.8
	Overall	28672	17.0	16.5	-0.4	2.8	-1.4	9.0
JUN.-SEP.	Global	1377	41.9	40.6	-1.3	2.2	-3.1	5.2
	Diffuse	1377	24.2	21.7	-2.4	4.1	-5.8	9.8
	Beam	1377	17.7	18.8	1.1	2.6	2.7	6.3
	S90	1377	21.1	20.2	-0.9	2.4	-2.1	5.8
	W90	1377	18.4	17.7	-0.7	3.6	-1.7	8.6
	E90	1377	17.3	16.9	-0.5	3.4	-1.1	8.2
	N90	1377	9.1	9.7	0.6	2.6	1.4	6.2
	Overall	9639	21.4	20.8	-0.6	3.1	-1.4	7.3
DEC.-MAR.	Global	1314	20.9	20.7	-0.2	0.8	-1.2	3.8
	Diffuse	1314	12.9	12.3	-0.6	1.8	-3.1	8.5
	Beam	1314	8.0	8.4	0.4	1.7	1.9	7.9
	S90	1314	21.3	20.9	-0.3	5.0	-1.6	23.7
	W90	1314	11.5	10.9	-0.6	2.0	-2.9	9.7
	E90	1314	10.4	9.7	-0.8	1.9	-3.6	8.9
	N90	1314	5.2	5.3	0.0	1.3	0.2	6.3
	Overall	9198	12.9	12.6	-0.3	2.4	-1.5	11.5
GENEVA (MOD. = HELIOSAT Version 7)								
YEAR	Global	4096	31.4	33.1	1.7	12.3	5.5	39.3
	Diffuse	4096	18.9	18.2	-0.8	8.1	-2.4	25.8
	Beam	4096	12.4	14.9	2.5	11.8	7.9	37.7
	S90	4096	20.3	23.5	3.2	13.6	10.2	43.2
	W90	4096	14.8	15.3	0.6	9.7	1.8	30.9
	E90	4096	13.6	14.6	1.0	9.0	3.2	28.8
	N90	4096	7.3	8.0	0.8	3.6	2.5	11.4
	Overall	28672	17.0	18.2	1.3	10.2	4.1	32.6
JUN.-SEP.	Global	1377	41.9	43.1	1.2	14.5	2.9	34.7
	Diffuse	1377	24.2	21.6	-2.6	9.5	-6.1	22.7
	Beam	1377	17.7	21.5	3.8	14.1	9.1	33.7
	S90	1377	21.1	22.0	0.9	8.4	2.2	20.1
	W90	1377	18.4	19.1	0.6	11.5	1.5	27.4
	E90	1377	17.3	18.2	0.9	9.3	2.1	22.2
	N90	1377	9.1	9.6	0.5	4.3	1.3	10.2
	Overall	9639	21.4	22.2	0.8	10.7	1.9	25.7
DEC.-MAR.	Global	1314	20.9	22.4	1.5	7.7	7.2	36.7
	Diffuse	1314	12.9	13.9	1.0	5.6	4.9	26.8
	Beam	1314	8.0	8.5	0.5	7.8	2.3	37.3
	S90	1314	21.3	24.4	3.1	15.1	14.9	72.3
	W90	1314	11.5	11.9	0.4	7.8	2.0	37.5
	E90	1314	10.4	10.9	0.5	7.2	2.5	34.4
	N90	1314	5.2	6.1	0.8	2.3	4.0	10.9
	Overall	9198	12.9	14.0	1.1	8.4	5.4	40.3

Table 1 Observed (OBS.) and modelled (MOD.) average half-hourly illuminances on a horizontal surface (Global, Diffuse, Beam), on four verticals (S90, W90, E90, N90), and for all these 7 parameters collectively (Overall). Mean Bias Deviations (MBD) and Root Mean Square Deviations (RMSD) are given, both in klux and as % of the observed global illuminances, together with the number (N) of half-hourly values. Illuminances are modelled with surface based and Heliosat based [Versions 7, 8 (Linke turbidity 3.0), and 8* (monthly turbidity); see text] horizontal irradiances as input.

Table 1 Continue

GENEVA (MOD. = HELIOSAT Version 8)								
		N	OBS.	MOD.	MBD	RMSD	MBD	RMSD
			(klux)		(klux)		(%)	
YEAR	Global	4094	31.4	33.2	1.9	12.3	5.9	39.2
	Diffuse	4094	18.9	18.2	-0.8	8.1	-2.5	25.9
	Beam	4094	12.4	15.1	2.6	11.9	8.4	37.9
	S90	4094	20.3	23.2	2.9	13.4	9.2	42.8
	W90	4094	14.8	15.7	0.9	9.6	2.9	30.7
	E90	4094	13.6	15.1	1.5	9.2	4.9	29.4
	N90	4094	7.3	8.1	0.8	3.6	2.6	11.3
	Overall	28658	16.9	18.3	1.4	10.2	4.5	32.6
JUN.-SEP.	Global	1376	41.8	44.1	2.2	14.5	5.3	34.7
	Diffuse	1376	24.2	22.1	-2.1	9.4	-5.0	22.5
	Beam	1376	17.7	22.0	4.3	14.2	10.3	34.0
	S90	1376	21.1	22.3	1.3	8.5	3.0	20.2
	W90	1376	18.4	20.1	1.7	11.6	4.0	27.7
	E90	1376	17.3	19.3	2.0	9.5	4.7	22.7
	N90	1376	9.1	9.9	0.8	4.2	1.9	10.1
	Overall	9632	21.4	22.8	1.5	10.8	3.5	25.8
DEC.-MAR.	Global	1314	20.9	21.5	0.6	7.8	2.7	37.1
	Diffuse	1314	12.9	13.2	0.3	5.7	1.4	27.5
	Beam	1314	8.0	8.3	0.3	7.9	1.3	37.7
	S90	1314	21.3	23.4	2.1	15.0	10.2	71.7
	W90	1314	11.5	11.5	0.0	7.9	0.2	37.7
	E90	1314	10.4	10.9	0.5	7.2	2.2	34.4
	N90	1314	5.2	5.8	0.5	2.3	2.5	11.1
	Overall	9198	12.9	13.5	0.6	8.4	2.9	40.4
GENEVA (MOD. = HELIOSAT Version 8*)								
YEAR	Global	4094	31.4	31.9	0.5	11.9	1.6	38.1
	Diffuse	4094	18.9	18.6	-0.3	8.0	-1.0	25.7
	Beam	4094	12.4	13.2	0.8	11.0	2.6	35.1
	S90	4094	20.3	22.5	2.2	13.4	7.0	42.7
	W90	4094	14.8	15.2	0.4	9.6	1.3	30.5
	E90	4094	13.6	14.2	0.6	8.7	1.9	27.6
	N90	4094	7.3	8.2	1.0	3.7	3.1	11.8
	Overall	28658	16.9	17.7	0.7	9.9	2.4	31.6
JUN.-SEP.	Global	1376	41.8	41.2	-0.6	13.7	-1.5	32.8
	Diffuse	1376	24.2	23.0	-1.2	9.3	-2.8	22.2
	Beam	1376	17.7	18.3	0.6	12.5	1.4	29.9
	S90	1376	21.1	20.9	-0.2	8.0	-0.5	19.0
	W90	1376	18.4	18.7	0.3	11.1	0.8	26.5
	E90	1376	17.3	17.6	0.3	8.6	0.7	20.7
	N90	1376	9.1	10.2	1.1	4.4	2.6	10.6
	Overall	9632	21.4	21.4	0.0	10.1	0.1	24.1
DEC.-MAR.	Global	1314	20.9	21.5	0.6	7.8	2.7	37.1
	Diffuse	1314	12.9	13.2	0.3	5.7	1.4	27.5
	Beam	1314	8.0	8.3	0.3	7.9	1.3	37.7
	S90	1314	21.3	23.8	2.5	16.0	12.2	76.4
	W90	1314	11.5	11.8	0.3	8.2	1.4	39.3
	E90	1314	10.4	10.6	0.2	7.4	0.8	35.5
	N90	1314	5.2	5.9	0.6	2.4	2.9	11.6
	Overall	9198	12.9	13.6	0.7	8.8	3.3	42.0

GÄVLE (MOD. = SURFACE)								
		N	OBS.	MOD.	MBD	RMSD	MBD	RMSD
			(klux)		(klux)		(%)	
YEAR	Global	1687	42.9	40.9	-1.9	2.5	-4.5	5.7
	Diffuse	1650	20.7	20.4	-0.3	1.2	-0.7	2.9
	Beam	1686	22.6	20.7	-2.0	3.7	-4.6	8.6
	S90	1686	31.8	30.2	-1.6	3.0	-3.8	6.9
	W90	1676	23.2	23.1	-0.1	3.2	-0.3	7.5
	E90	1687	17.2	17.0	-0.3	2.4	-0.6	5.6
	N90	1687	8.7	9.5	0.8	2.5	1.8	5.8
	Overall	11759	23.9	23.1	-0.8	2.7	-1.8	6.4
NO SNOW	Global	1620	43.7	41.8	-2.0	2.5	-4.5	5.7
	Diffuse	1586	21.1	20.7	-0.3	1.2	-0.7	2.9
	Beam	1619	23.1	21.1	-2.0	3.7	-4.5	8.4
	S90	1620	31.9	30.2	-1.6	2.9	-3.8	6.6
	W90	1609	23.5	23.5	-0.1	3.1	-0.2	7.1
	E90	1620	17.6	17.3	-0.2	2.4	-0.6	5.5
	N90	1620	8.8	9.6	0.8	2.5	1.9	5.7
	Overall	11294	24.2	23.5	-0.8	2.7	-1.8	6.2
"SNOW"	Global	67	22.2	21.1	-1.1	1.9	-5.0	8.7
	Diffuse	64	11.6	11.4	-0.2	0.8	-0.9	3.5
	Beam	67	11.1	9.3	-1.8	4.1	-8.1	18.4
	S90	66	30.3	28.8	-1.5	4.4	-6.8	19.8
	W90	67	15.0	13.5	-1.5	5.1	-6.8	23.1
	E90	67	9.9	9.3	-0.7	1.9	-3.0	8.4
	N90	67	5.4	5.0	-0.4	1.3	-1.8	6.0
	Overall	465	15.1	14.0	-1.0	3.2	-4.7	14.5
GÄVLE (MOD. = HELIOSAT Version 7)								
YEAR	Global	1687	42.9	40.2	-2.6	9.6	-6.2	22.3
	Diffuse	1650	20.7	20.9	0.2	7.2	0.6	16.8
	Beam	1686	22.6	19.4	-3.2	11.5	-7.6	26.8
	S90	1686	31.8	29.3	-2.5	9.6	-5.9	22.4
	W90	1676	23.2	22.3	-0.9	9.7	-2.1	22.6
	E90	1687	17.2	16.8	-0.4	6.3	-1.0	14.7
	N90	1687	8.7	9.6	1.0	3.3	2.2	7.6
	Overall	11759	23.9	22.7	-1.2	8.5	-2.8	19.9
NO SNOW	Global	1620	43.7	41.2	-2.5	9.7	-5.8	22.1
	Diffuse	1586	21.1	21.3	0.3	7.2	0.7	16.6
	Beam	1619	23.1	20.0	-3.2	11.5	-7.2	26.3
	S90	1620	31.9	29.6	-2.3	9.2	-5.2	21.0
	W90	1609	23.5	22.8	-0.8	9.7	-1.7	22.2
	E90	1620	17.6	17.2	-0.4	6.4	-0.8	14.6
	N90	1620	8.8	9.8	1.0	3.3	2.3	7.5
	Overall	11294	24.2	23.1	-1.1	8.5	-2.5	19.5
"SNOW"	Global	67	22.2	17.2	-4.9	7.1	-22.2	32.1
	Diffuse	64	11.6	10.6	-1.0	5.6	-4.5	25.0
	Beam	67	11.1	6.0	-5.1	10.9	-23.0	49.0
	S90	66	30.3	21.5	-8.8	17.2	-39.7	77.6
	W90	67	15.0	10.9	-4.1	8.6	-18.3	38.6
	E90	67	9.9	7.8	-2.1	4.9	-9.7	22.3
	N90	67	5.4	4.9	-0.5	1.7	-2.3	7.9
	Overall	465	15.1	11.3	-3.8	9.2	-17.1	41.6

Table 2 Same as Table 1 for hourly values at Gävle, for the entire year, for snow-free periods, and for possibly snow affected periods. Illuminances are modelled with surface based and Heliosat based (Versions 7, 8, and 9) horizontal irradiances as input.

Table 2 Continue

GÄVLE (MOD. = HELIOSAT Version 8)								
		N	OBS.	MOD.	MBD	RMSD	MBD	RMSD
			(klux)		(klux)		(%)	
YEAR	Global	1687	42.9	40.7	-2.1	9.3	-4.9	21.6
	Diffuse	1650	20.7	21.3	0.6	6.9	1.4	16.1
	Beam	1686	22.6	19.6	-3.1	11.5	-7.1	26.8
	S90	1686	31.8	29.4	-2.4	9.6	-5.6	22.4
	W90	1676	23.2	22.9	-0.3	9.5	-0.7	22.1
	E90	1687	17.2	17.5	0.2	5.7	0.5	13.4
	N90	1687	8.7	9.8	1.2	3.1	2.7	7.3
	Overall	11759	23.9	23.0	-0.8	8.4	-2.0	19.5
NO SNOW	Global	1620	43.7	41.7	-2.0	9.3	-4.6	21.4
	Diffuse	1586	21.1	21.7	0.7	6.9	1.5	15.9
	Beam	1619	23.1	20.1	-3.0	11.5	-6.8	26.3
	S90	1620	31.9	29.8	-2.1	9.1	-4.8	20.8
	W90	1609	23.5	23.4	-0.2	9.5	-0.4	21.7
	E90	1620	17.6	17.9	0.3	5.8	0.7	13.2
	N90	1620	8.8	10.0	1.2	3.2	2.8	7.3
	Overall	11294	24.2	23.5	-0.7	8.3	-1.7	19.0
″SNOW″	Global	67	22.2	17.1	-5.1	7.1	-22.9	32.2
	Diffuse	64	11.6	10.5	-1.1	5.5	-4.9	24.7
	Beam	67	11.1	5.9	-5.2	10.9	-23.3	49.2
	S90	66	30.3	21.0	-9.4	17.9	-42.3	80.8
	W90	67	15.0	10.8	-4.2	8.5	-18.9	38.5
	E90	67	9.9	7.9	-2.0	4.5	-9.2	20.3
	N90	67	5.4	4.9	-0.6	1.7	-2.5	7.6
	Overall	465	15.1	11.1	-3.9	9.4	-17.8	42.3

GÄVLE (MOD. = HELIOSAT Version 9)								
YEAR	Global	1687	42.9	42.2	-0.7	9.1	-1.6	21.3
	Diffuse	1650	20.7	21.9	1.2	7.1	2.9	16.5
	Beam	1686	22.6	20.4	-2.3	11.2	-5.3	26.0
	S90	1686	31.8	30.7	-1.1	9.2	-2.6	21.4
	W90	1676	23.2	23.6	0.4	9.3	0.9	21.8
	E90	1687	17.2	17.8	0.6	5.8	1.3	13.5
	N90	1687	8.7	10.1	1.5	3.2	3.4	7.6
	Overall	11759	23.9	23.8	-0.1	8.2	-0.2	19.2
NO SNOW	Global	1620	43.7	43.1	-0.6	9.2	-1.3	21.1
	Diffuse	1586	21.1	22.3	1.3	7.2	3.0	16.4
	Beam	1619	23.1	20.9	-2.2	11.2	-5.0	25.6
	S90	1620	31.9	31.0	-0.9	8.7	-2.0	20.0
	W90	1609	23.5	24.1	0.5	9.4	1.3	21.5
	E90	1620	17.6	18.2	0.6	5.8	1.5	13.4
	N90	1620	8.8	10.3	1.5	3.3	3.5	7.5
	Overall	11294	24.2	24.3	0.1	8.2	0.1	18.8
″SNOW″	Global	67	22.2	18.3	-3.8	6.2	-17.3	28.2
	Diffuse	64	11.6	11.4	-0.2	4.7	-0.8	21.3
	Beam	67	11.1	6.4	-4.7	10.4	-21.4	47.0
	S90	66	30.3	22.7	-7.6	16.5	-34.2	74.3
	W90	67	15.0	11.5	-3.5	7.9	-15.6	35.7
	E90	67	9.9	8.3	-1.6	4.3	-7.2	19.4
	N90	67	5.4	5.2	-0.2	1.3	-0.9	5.9
	Overall	465	15.1	12.0	-3.1	8.7	-14.0	39.0

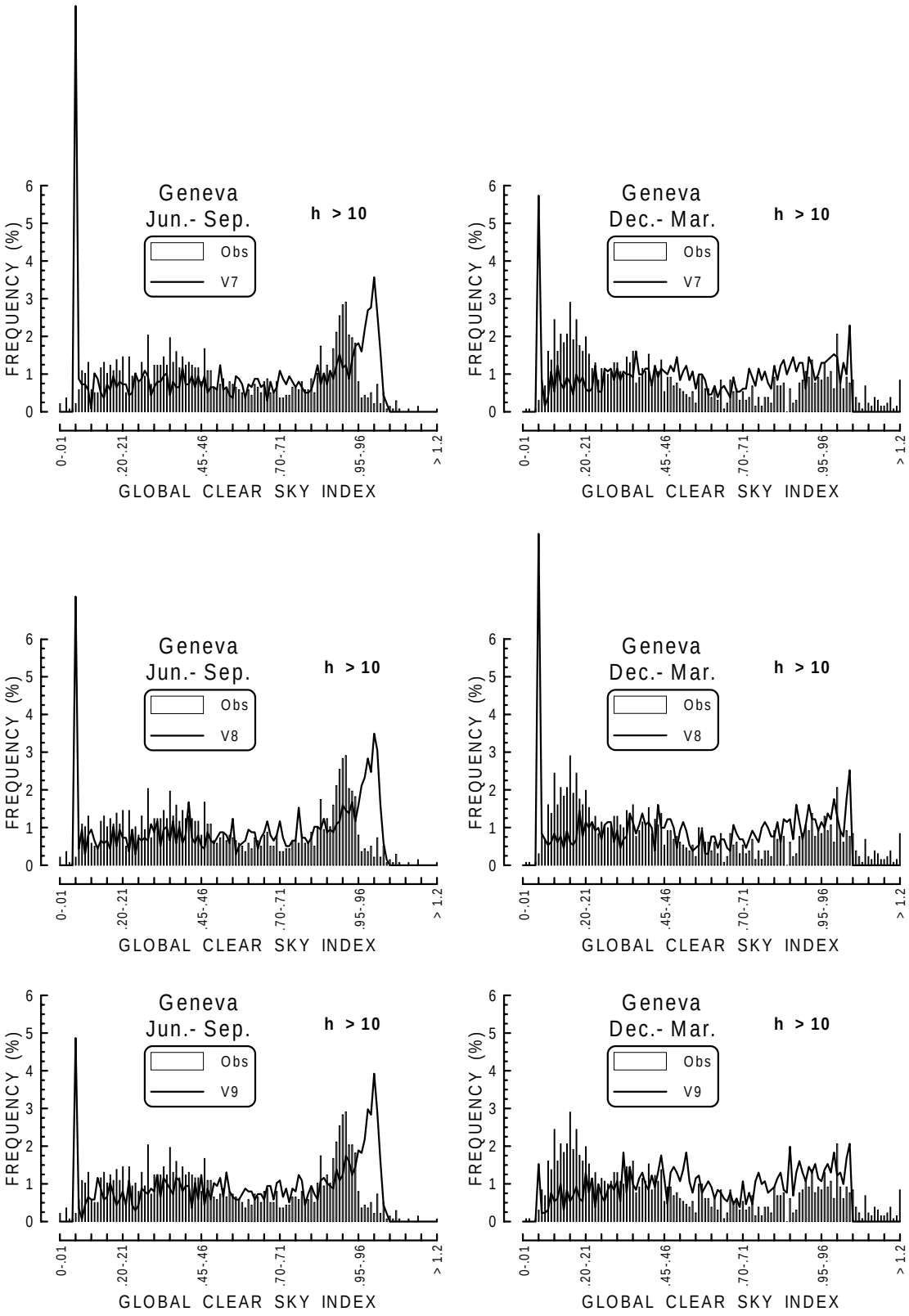

Fig. 1a) Observed (histograms) and modelled (curves) frequency distributions of half-hourly global clear sky indices for solar elevation above 10° for the summer (left) and the winter (right) at Geneva. The modelled values are obtained by Heliosat Versions 7 (top), 8 (middle), and 9 (bottom).

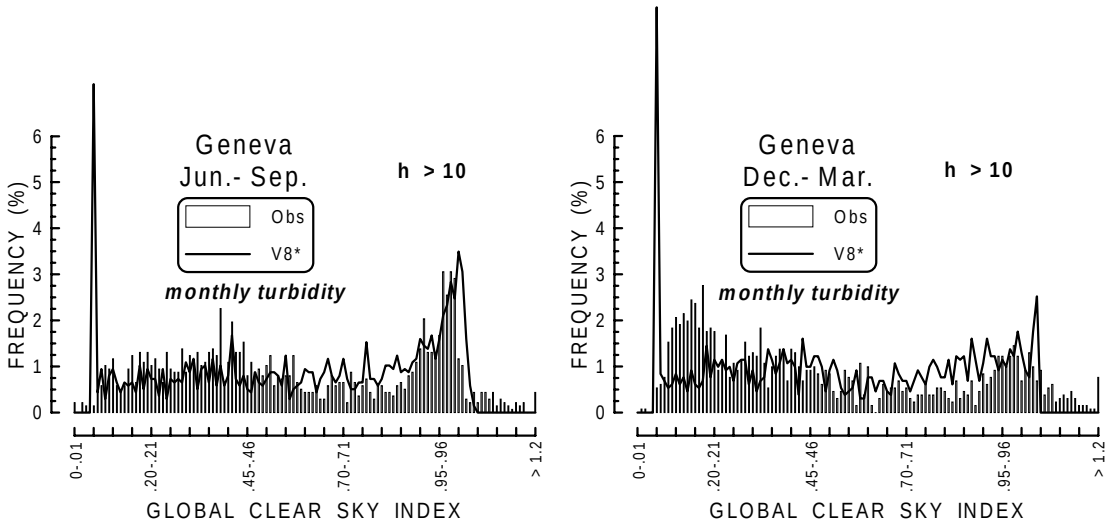

Fig. 1b) Same as Fig. 1a), but for Version 8* (V8*, clear sky model with climatological monthly Linke turbidities; see text).

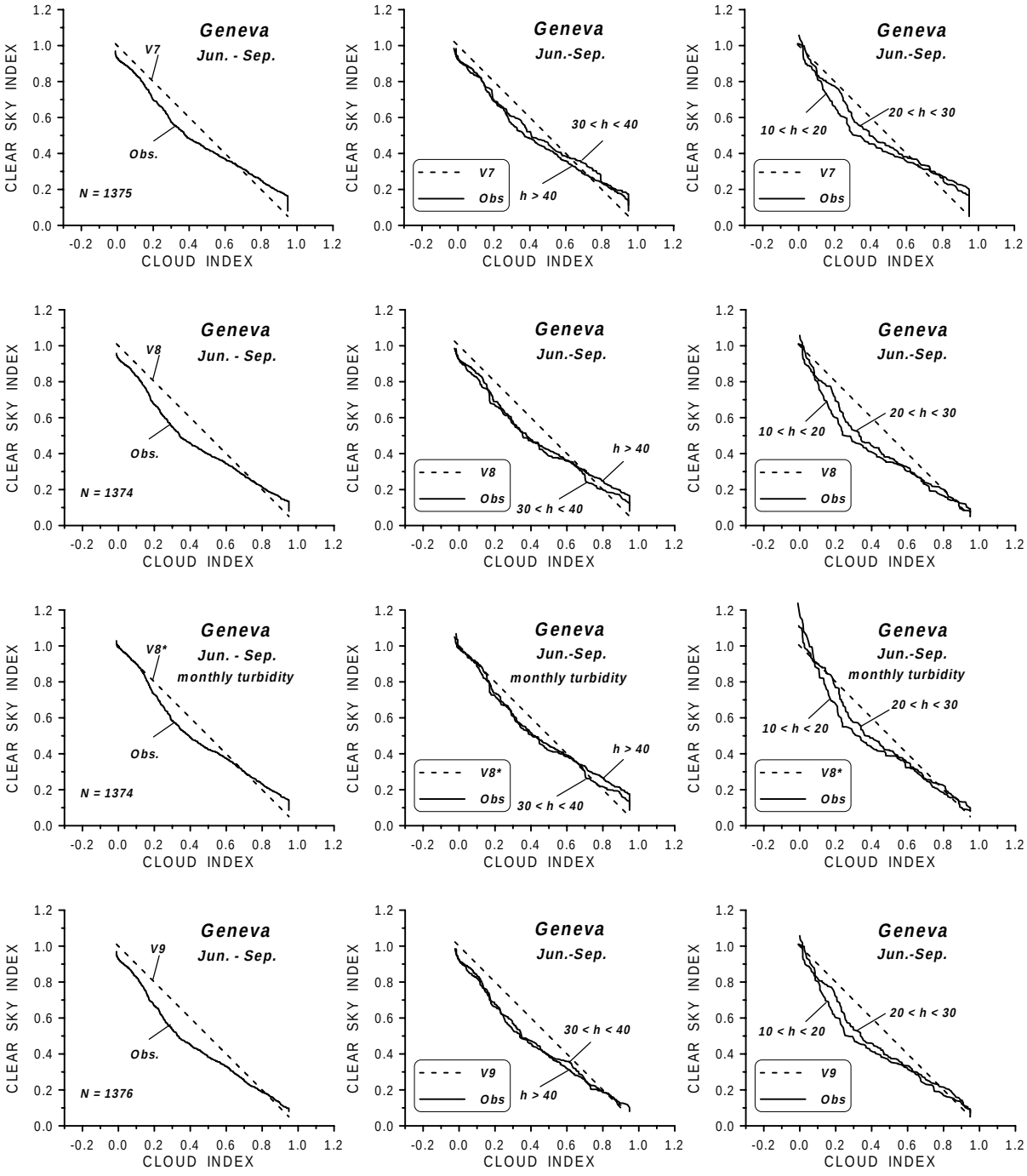

Fig. 2a) "Percentile match curves" between half-hourly clear sky index (observed and modelled from Heliosat Versions 7, 8, and 9) and cloud index (modelled from the respective Heliosat Versions) for the period June-September at Geneva. Curves are given for all hours (left column) and for different solar elevation (h) intervals (middle and right columns). Curves are drawn for the central 95% of the distributions. For Version 8, results are shown both for the clear sky model with a fixed Linke turbidity coefficient 3.0 (V8) and with climatological monthly turbidity coefficients (V8*).

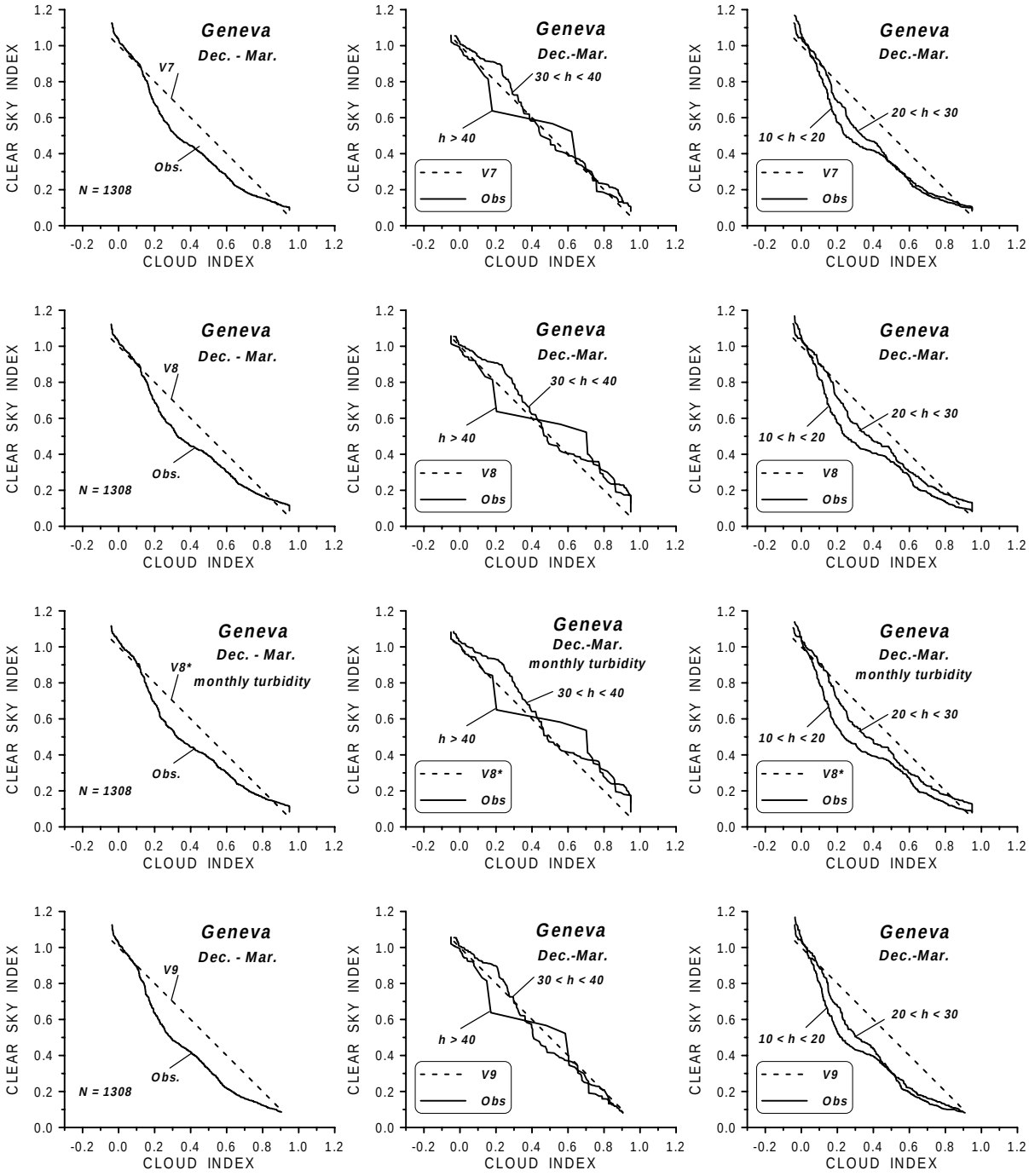

Fig. 2b) Same as Fig. 2a), but for the period December-March at Geneva.

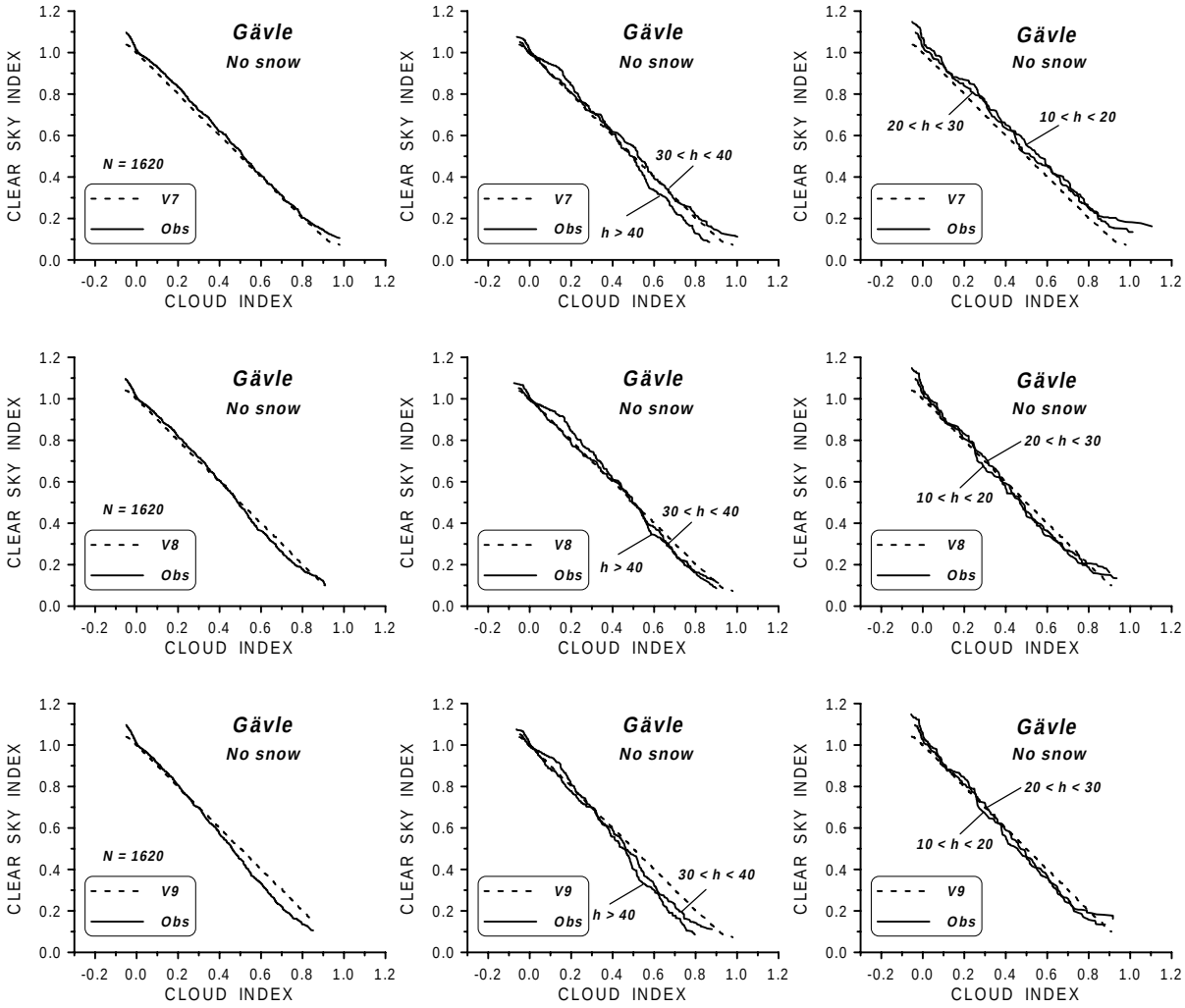

Fig. 2c) Same as Fig. 2a), but for hourly values at snow-free conditions at Gävle.

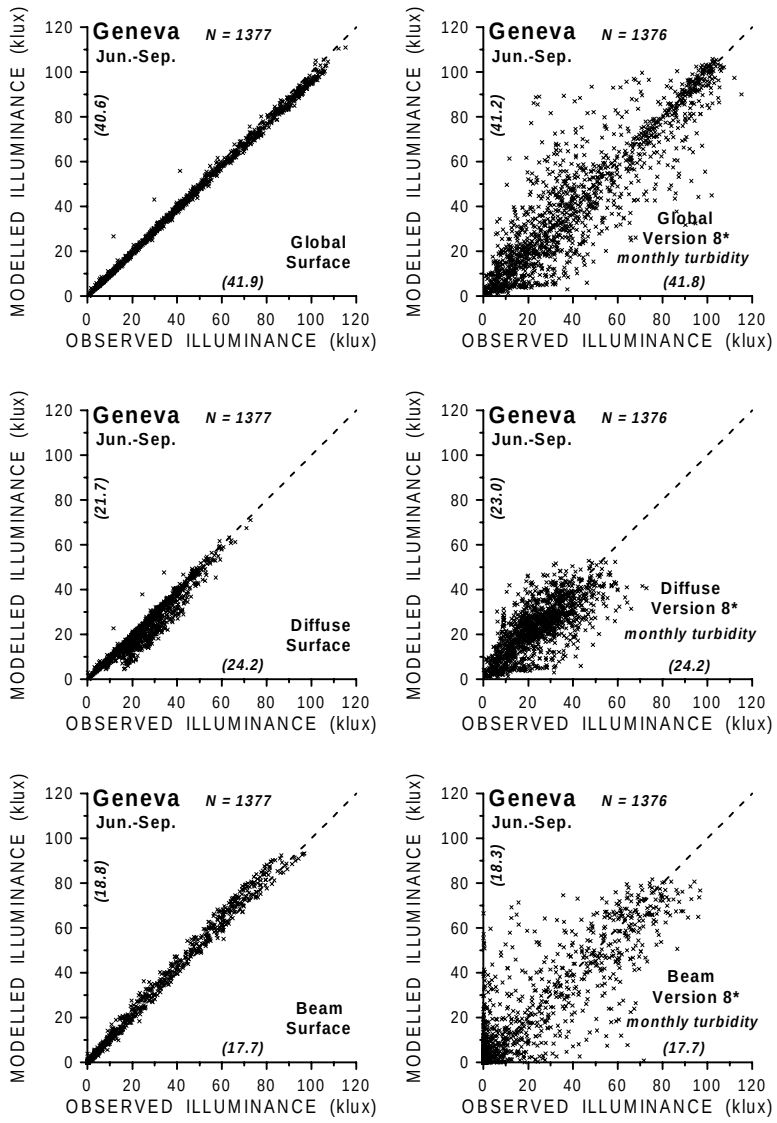

Fig. 3a) Observed vs modelled global, beam, and diffuse horizontal half-hourly illuminances for June - September at Geneva. Illuminances are modelled from surface observed (left column) or from Heliosat Version 8* with climatological monthly Linke turbidities in the clear sky model (right column) horizontal irradiances. The number of values (N) are given together with observed and modelled averages (in parentheses along the axes).

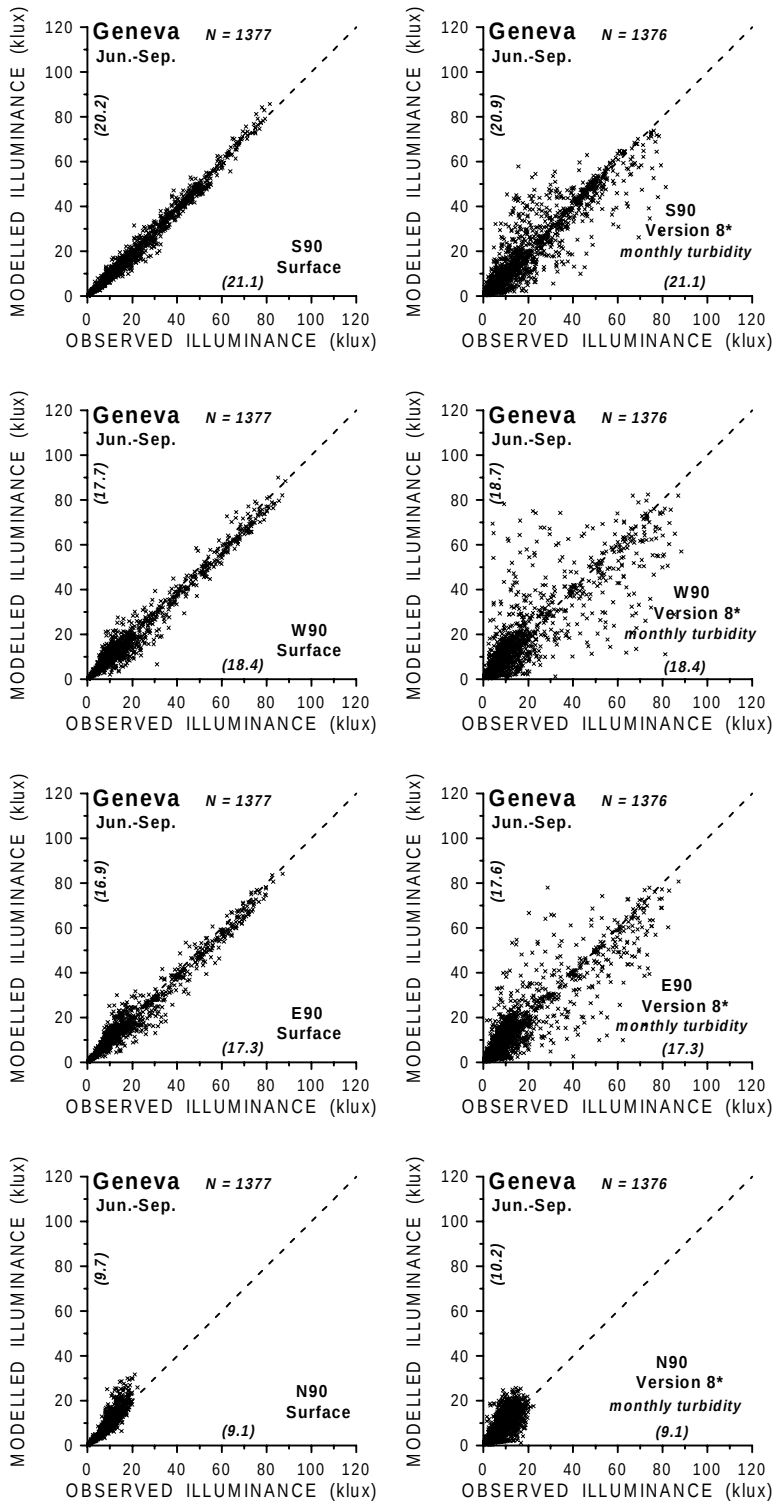

Fig. 3b) Same as Fig. 3a but for vertical surfaces facing south (S90), west (W90), east (E90), and north (N90). Illuminances are modelled from horizontal irradiances using foreground albedo A=0.1.

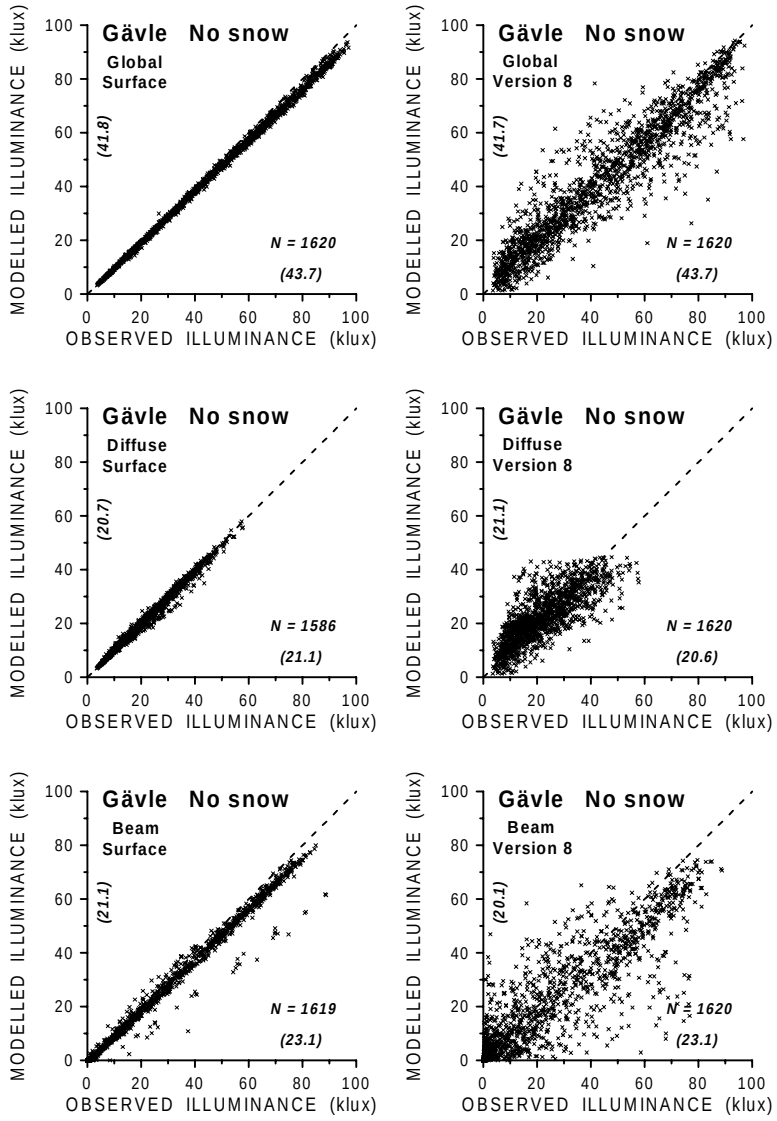

Fig. 4a) Same as Fig. 3a), but for snow-free conditions at Gävle.

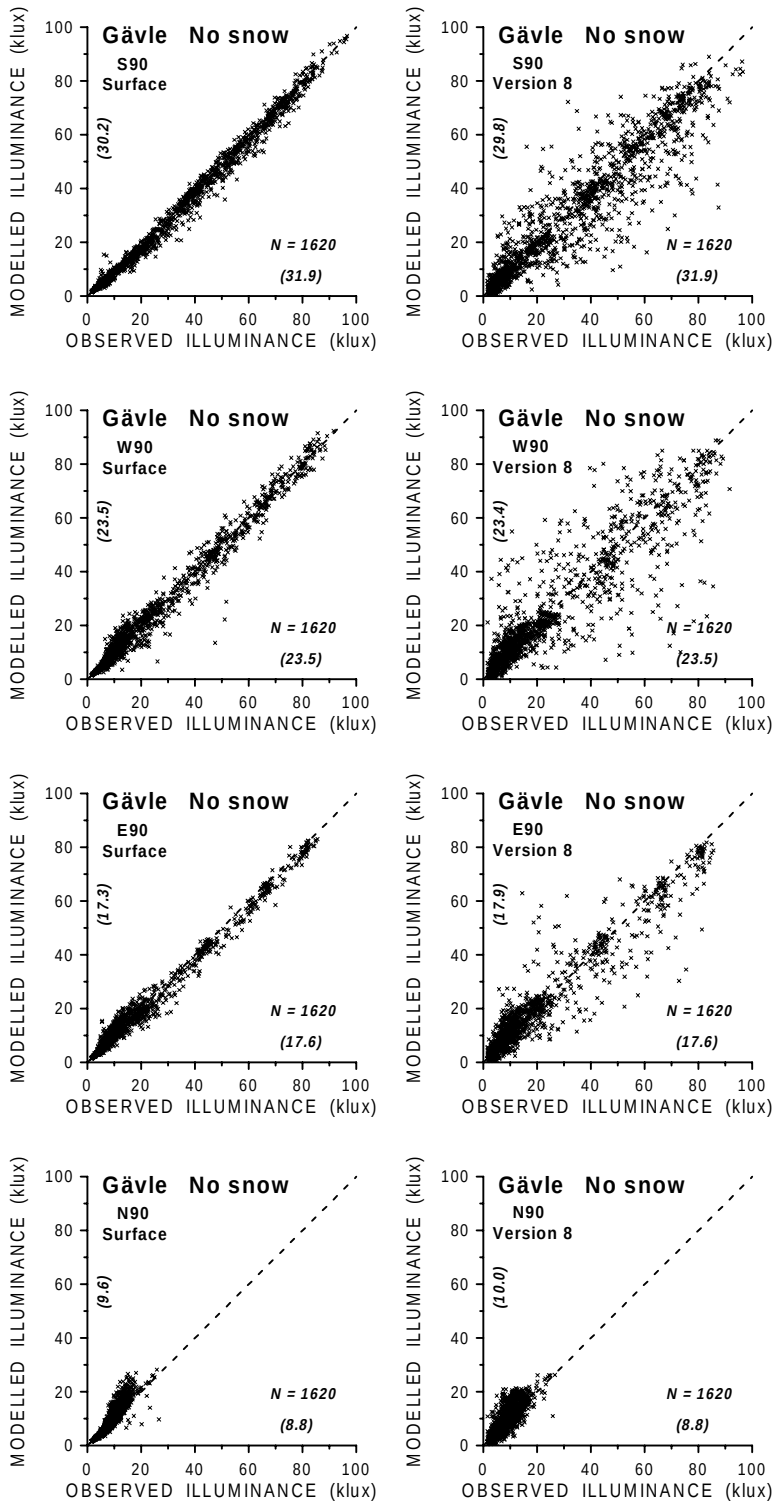

Fig. 4b) Same as Fig. 3b but for snow-free conditions at Gävle.

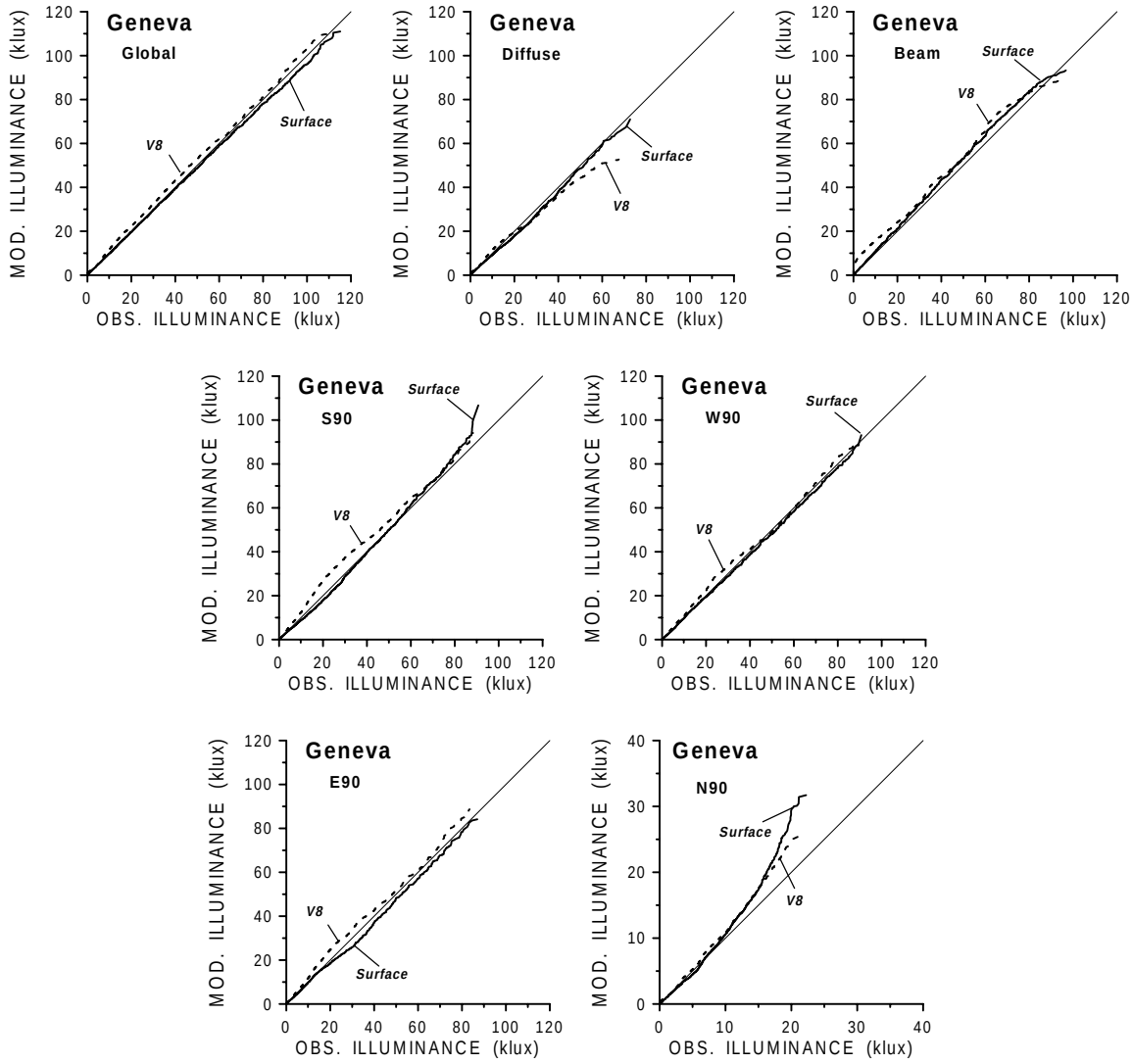

Fig. 5a ″Percentile match curves″ between observed and modelled global, diffuse, and horizontal beam illuminance (upper row), and illuminances on vertical surfaces facing south (S90), west (W90), east (E90), and north (N90) for the whole year at Geneva. Illuminances are modelled from surface observed (Surface) and Heliosat Version 8 (V8) horizontal irradiances with foreground albedo A=0.1. The 1 : 1 lines are also given. Note that the Y-axis for N90 deviates from the others.

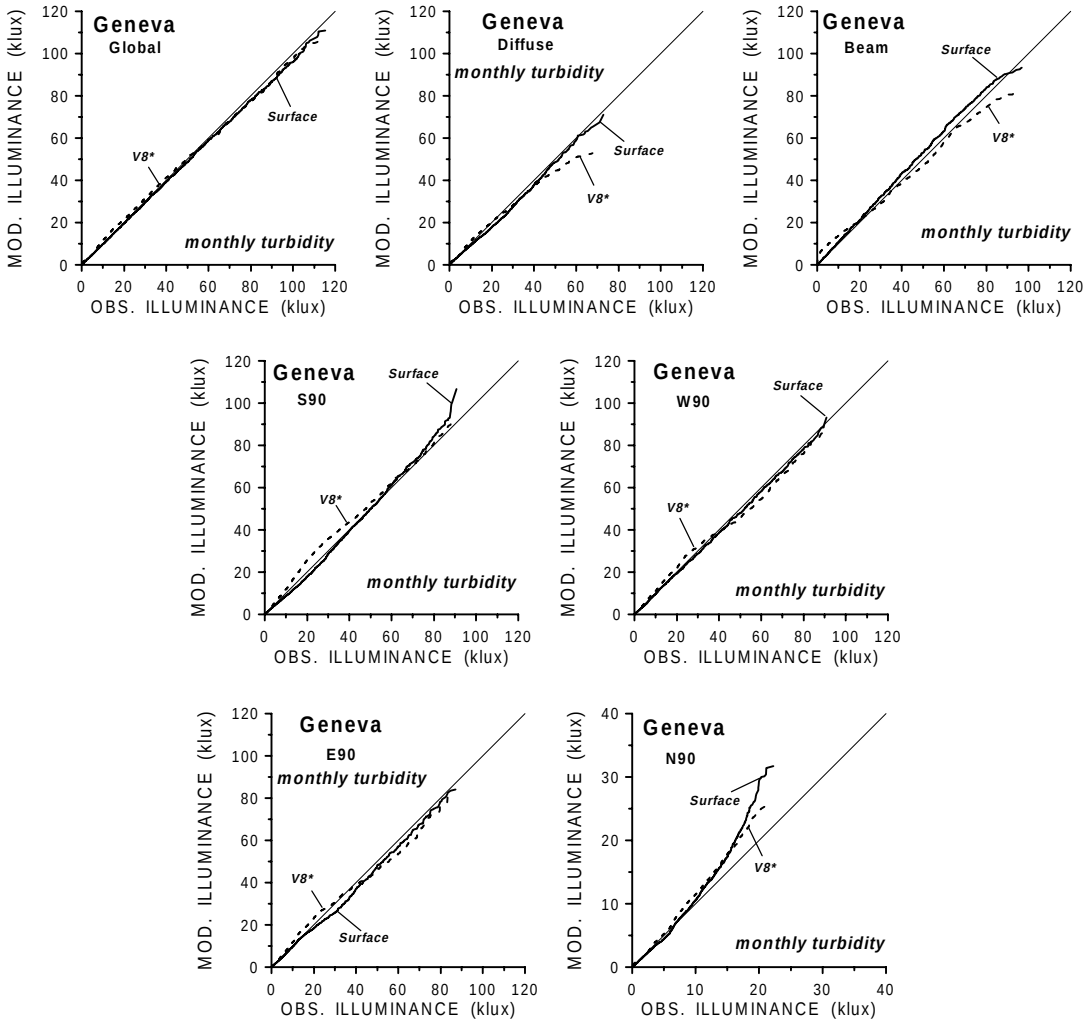

Fig. 5b) Same as Fig. 5a), but for Heliosat Version 8* (V8*) with climatological monthly Linke turbidities as input to the clear sky model.

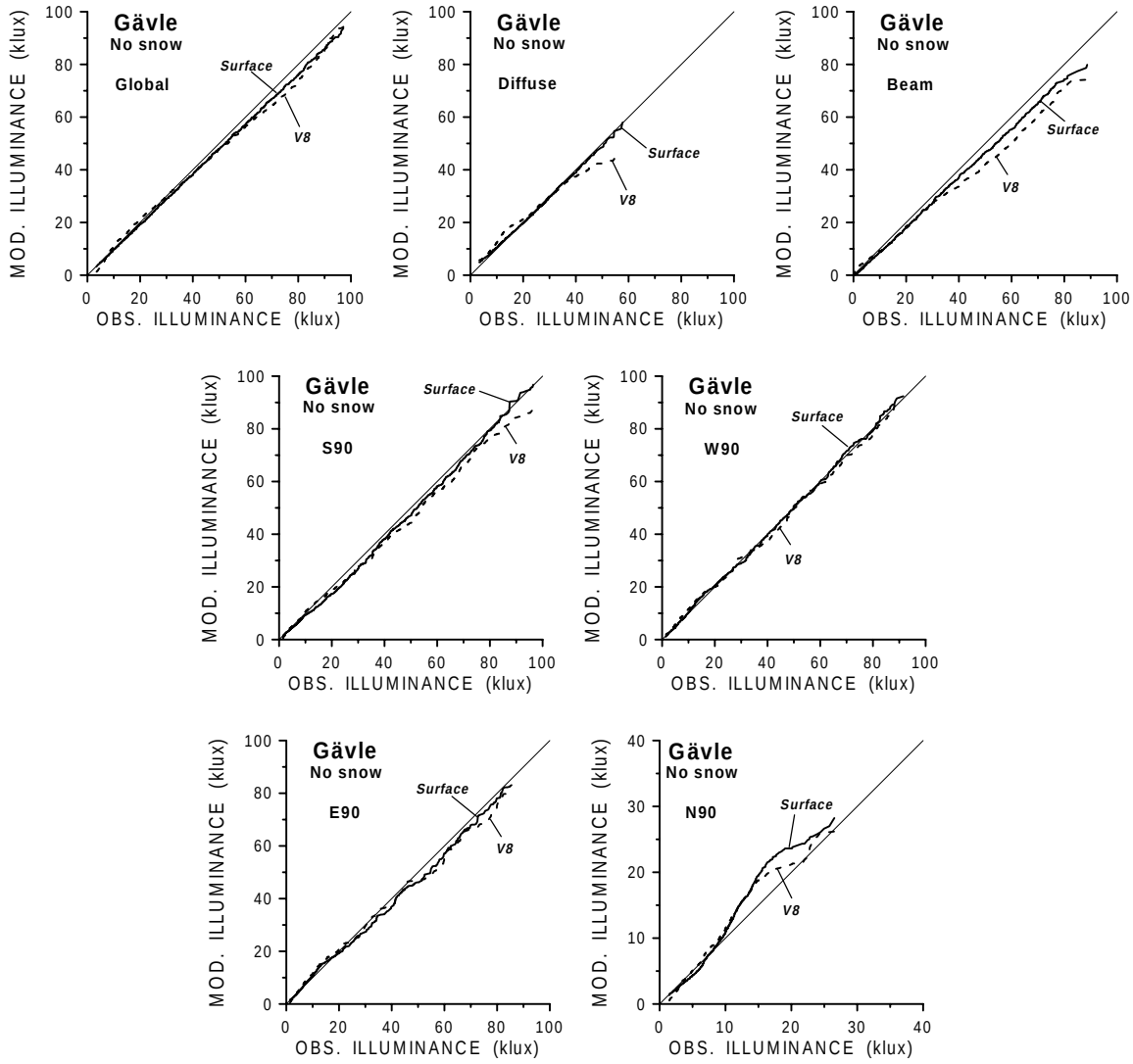

Fig. 5c) Same as Fig. 5a), but for the snow-free period at Gävle.

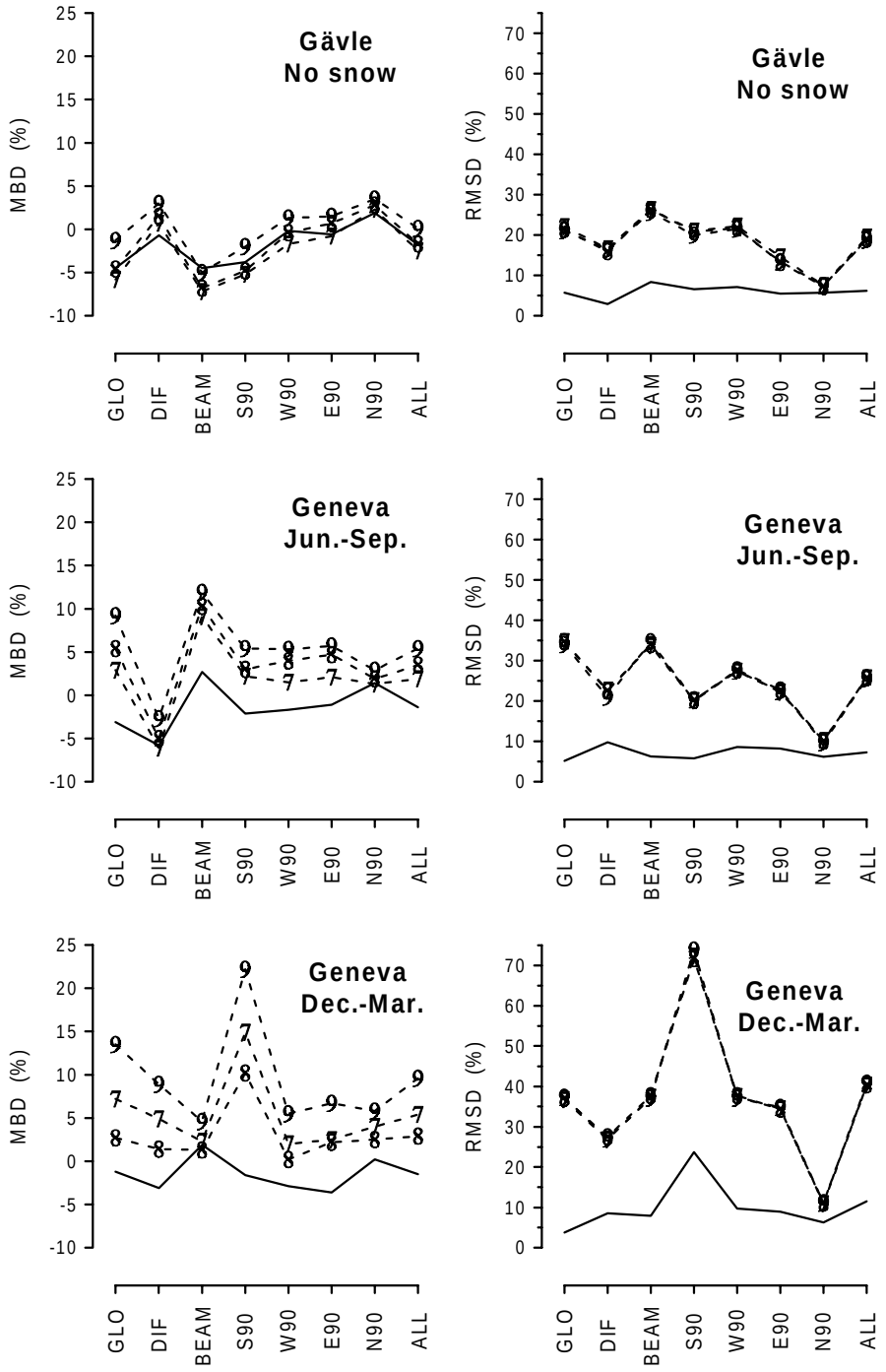

Fig. 6a) Mean Bias Deviation (MBD = modelled - observed, left) and Root Mean Square Deviation (RMSD, right) for snow-free situations at Gävle and for summer and winter at Geneva. Values are given for a horizontal surface (Global, Diffuse, and Beam), for 4 vertical surfaces (S90, W90, E90, and N90) and for all 7 parameters collectively (All). Fully drawn curves correspond to surface measured irradiances as input, while broken curves with numbers plotted correspond to Heliosat (Versions 7, 8, and 9) data as input. MBD's and RMSD's are given as percentages of the observed global illuminance.

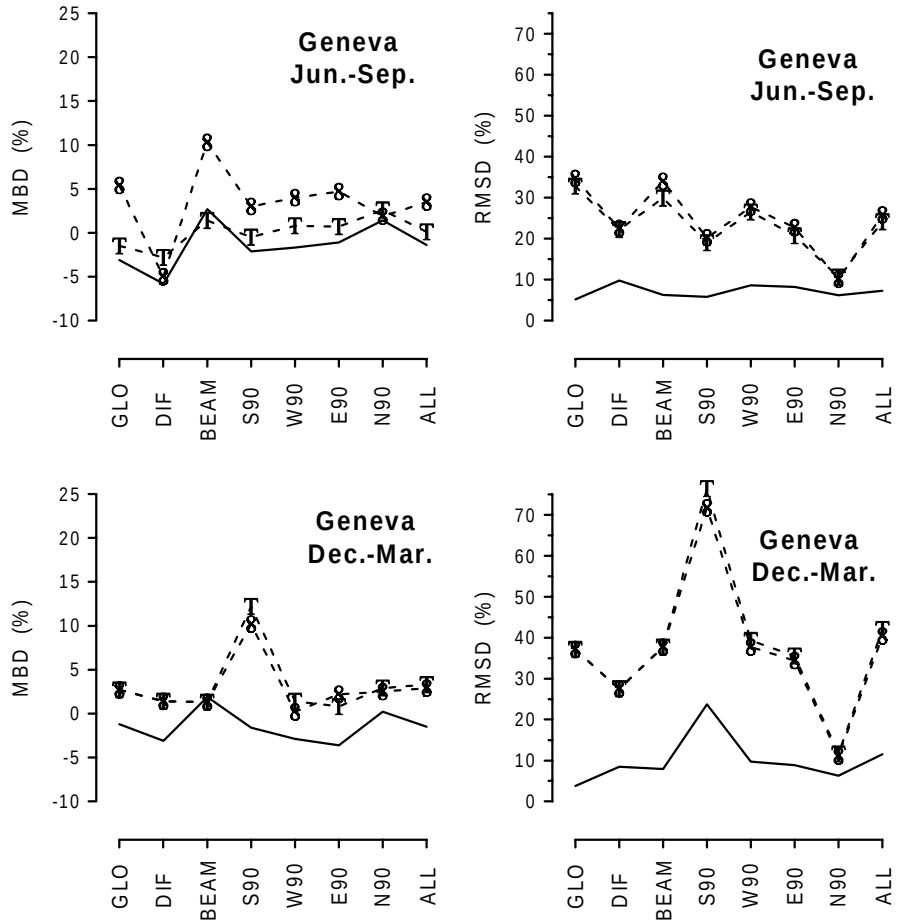

Fig. 6b) Same as Fig. 6a), but for surface measured irradiances (fully drawn curves) and Heliosat Version 8 irradiances (broken curves; clear sky model with Linke turbidity factor = 3.0 marked with 8, or climatological monthly turbidity factor, marked with T) as input for Geneva.